

## DOPED ZINC ALUMINATE SPINEL SYNTHESIZED BY HYDROTHERMAL METHOD

I. MIRON<sup>a,b\*</sup>, C. ENACHE<sup>c</sup>, I. GROZESCU<sup>a,b</sup>

<sup>a</sup>*"Politehnica" University of Timisoara, 300006, Timisoara, Romania*

<sup>b</sup>*National Institute for Research and Development in Electrochemistry and Condensed Matter Timisoara, 300569, Romania*

<sup>c</sup>*Institute of Chemistry Timisoara of Romanian Academy, 300223, Timisoara, Romania*

ZnAl<sub>2</sub>O<sub>4</sub> spinel doped with Eu<sup>3+</sup> ions was prepared by hydrothermal method. After hydrothermal treatment the sample was heated at 1000°C. X-ray diffraction analysis confirmed the high crystallinity and purity of the sample and the average crystallite size calculated from the pattern was smaller than 40 nm. Optical properties of ZnAl<sub>2-x</sub>O<sub>4</sub>:Eu<sub>x</sub> spinel were also determined. The band gap of ZnAl<sub>2-x</sub>O<sub>4</sub>:Eu<sub>x</sub> spinel was found to be around 3.89 eV. The PLE measurements monitored at two excitation wavelengths (253 nm and 395 nm) confirmed the high luminescent properties of the sample prepared by hydrothermal method and heated at 1000°C. The <sup>5</sup>D<sub>0</sub>→<sup>7</sup>F<sub>2</sub> red emission centered at 617 nm was the most intense one.

(Received April 4, 2012; Accepted July 5, 2012)

*Keywords:* Zinc aluminate, Hydrothermal method, Europium, Spinel

### 1. Introduction

During the last decades, attention of the most researchers has been focused on the synthesis of different nanocrystals with sizes ranging from 1 to 100 nm [1]. This type of nanocrystals presents interest due to the interesting size-dependent electrical, optical, magnetic and chemical properties in comparison with those of bulk crystals [2].

Spinel type materials have long been a topic of interest because they may exhibit different sizes depending on synthesis type. Also, they can be used as magnetic materials, pigments, catalyst and refractory materials [3]. Among them, zinc aluminate spinel is of interest due to its properties such as high mechanical resistance, high thermal stability, low temperature sinterability, low surface acidity and good diffusion [4]. Zinc aluminate spinel is also transparent to light with wavelengths above 320 nm and is suitable for UV optoelectronic applications [5]. Zinc aluminate spinel has the normal spinel structure and the chemical formula of AB<sub>2</sub>O<sub>4</sub> in which Zn<sup>2+</sup> (A) ions occupy tetrahedral sites and Al<sup>3+</sup> (B) ions the octahedral sites. Many synthesis methods for the obtaining of ZnAl<sub>2</sub>O<sub>4</sub> have been reported, such as: co-precipitation [6,7], hydrothermal method [1,8,9], sol-gel [3,10], combustion synthesis [11]. Zinc aluminate spinel doped with rare earth metal ions has been investigated due to its luminescent properties. This properties results from its stability and high emission quantum yields [12,13]. Among rare-earths, europium is one of the best candidates for zinc aluminate spinels.

In the present paper, we report the hydrothermal synthesis of zinc aluminate spinels doped with Eu<sup>3+</sup> ions.

---

\*Corresponding author: mironiasmina@gmail.com

## 2. Experimental

ZnAl<sub>2</sub>O<sub>4</sub> spinel doped with Eu<sup>3+</sup> ions was prepared by hydrothermal method. Hydrothermal method synthesis involves mixing ions (nitrates, acetates or oxides) acting as oxidizing reagents with filler that acts as the reducing agent. Zinc nitrate hexahydrate (Zn(NO<sub>3</sub>)<sub>2</sub>·6H<sub>2</sub>O), aluminium nitrate nonahydrate (Al(NO<sub>3</sub>)<sub>3</sub>·9H<sub>2</sub>O) and europium chloride hydrate (EuCl<sub>3</sub>·xH<sub>2</sub>O) were used as precursors. As a precipitating agent water solution of ammonia (25%) was used. The precursors were dissolved in distilled water and the mixture was stirred on a magnetic stirrer. The appropriate amount of ammonia was added drop by drop till pH value became 8.5. The resulting suspension was transferred into a Teflon-lined stainless steel autoclave and sealed tightly then was introduced in an oven at 220°C for 8 h. A white precipitate resulted, which was then filtrated and washed many times with distilled water and ethylic alcohol, then dried in an oven at 100°C for 6 hours. After drying, a sufficient amount of resulting powder was treated thermally at 1000°C for 5h.

The characterization of the sample was achieved by X-ray powder diffractometer (PANalytical X'Pert Pro) with monochromatic Cu K $\alpha$  ( $k = 1.5418 \text{ \AA}$ ) incident radiation. The topography of the surface was achieved by atomic force microscope (Nanosurf<sup>®</sup> EasyScan 2 Advanced Research (AFM)). UV/VIS/NIR measurement was carried out using a UV/VIS/NIR spectrophotometer (Model Lambda 950). The photoluminescence (PLE) measurement was carried out using a spectrofluorophotometer at room temperature (Model LS55, Perkin Elmer).

## 3. Results and discussions

In Fig. 1 the X-ray diffraction patterns of zinc aluminate spinel doped with Eu<sup>3+</sup> ions synthesized by hydrothermal method are shown.

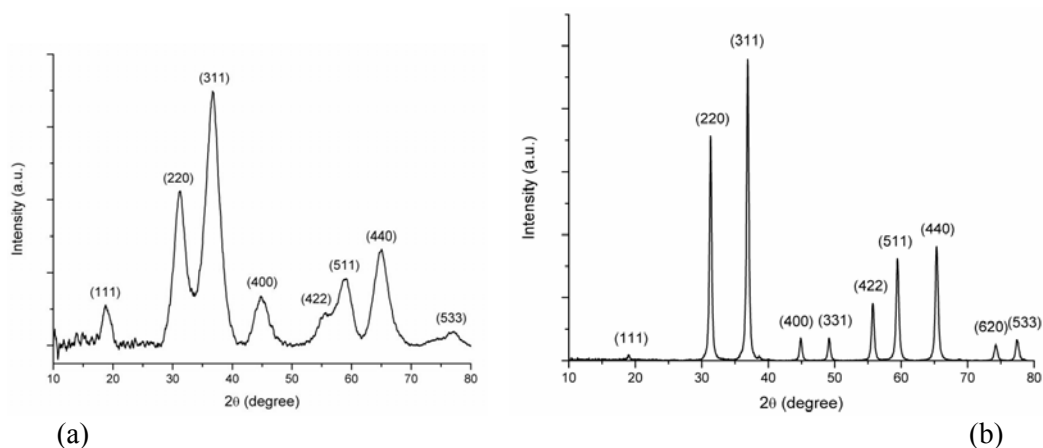


Fig. 1. X-ray diffraction pattern of ZnAl<sub>2</sub>O<sub>4</sub>:Eu: (a) as-prepared; (b) after annealing at 1000°C

As we can see, all the peaks observed in Fig. 1a are indexed as cubic ZnAl<sub>2</sub>O<sub>4</sub> (JCDs no. 05-0669). Moreover, all the peaks present remarkable broadening in comparison with standard probe. This means that our sample is characterized by small size crystallites. To demonstrate this affirmation we used Scherrer formula [14] to calculate the average crystallite size from X-ray line broadening ( $d_{311}$ ):

$$d = \frac{K\lambda}{(\beta^2 - \beta_0^2)^{1/2}} \cos \theta$$

where  $\beta$  is the half-width of the diffraction peak in radians,  $\beta_0$  corresponds to the instrumental broadening,  $K = 180/\pi$ ,  $\lambda$  is the X-ray wavelength, and  $\theta$  is the Bragg diffraction angle. The average crystallite size was found to be approximately 5.6 nm.

After annealing at 1000°C (Fig. 1b) the broadening of diffraction peaks is decreasing. In this case, as well, all the diffraction peaks correspond to those of the standard patterns of cubic zinc aluminate spinel (JCPDS no. 05-0669). No impurity presence was detected. As we can see the (311) peak present the highest intensity. The diffraction peaks in the patterns are indexed to spinel (space group Fd3m) phases. The average crystallite size was found to be approximately 37.1 nm which means that the particle size increases with the temperature.

Further, we will refer only to the sample treated thermally at 1000°C.

The atomic force microscopy was used to analyze the topography of the surface (Fig. 2). Scanning size was 1  $\mu\text{m}$  x 1  $\mu\text{m}$ . The sample was analyzed using the contact mode cantilever.

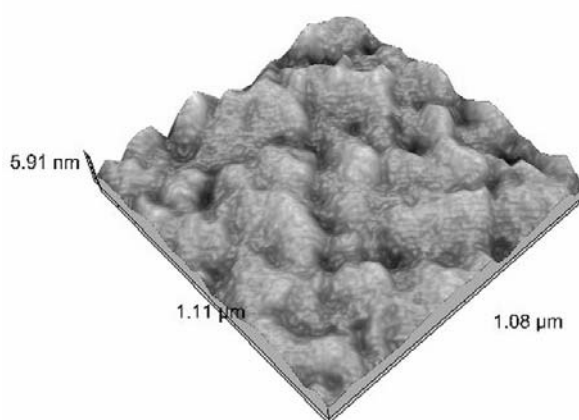


Fig. 2. AFM images of  $\text{ZnAl}_{2-x}\text{O}_4:\text{Eu}_x$

From the AFM measurements data, the average particle size was found to be approximately 34 nm. These measurements are in agreement with X-ray diffraction data. Because of the small sizes as we can see from AFM images sample present agglomerates.

To analyze chemical composition of the samples energy dispersive X-ray analysis (EDX) was performed. A typical EDX spectrum of  $\text{ZnAl}_2\text{O}_4:\text{Eu}$  is presented in Fig. 3.

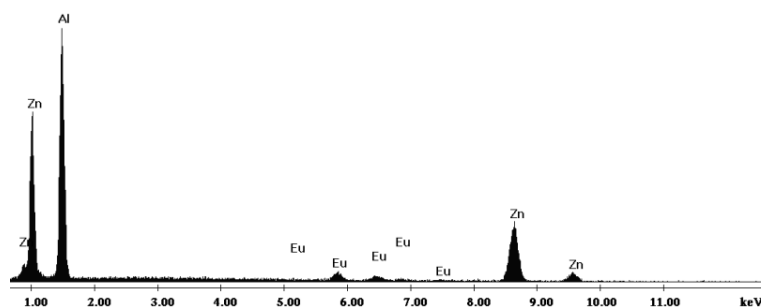


Fig. 3. The qualitative EDX analysis of  $\text{ZnAl}_{2-x}\text{O}_4:\text{Eu}_x$

One can see that no impurity was found in samples, only the Zn, Al and Eu elements. The results confirmed the purity of the obtained sample.

The optical absorbance spectrum was determined from the diffuse reflectance spectrum using Kubelka–Munk equation [15,16]. The optical absorbance spectrum was detected in the 250-485 nm region at room temperature.

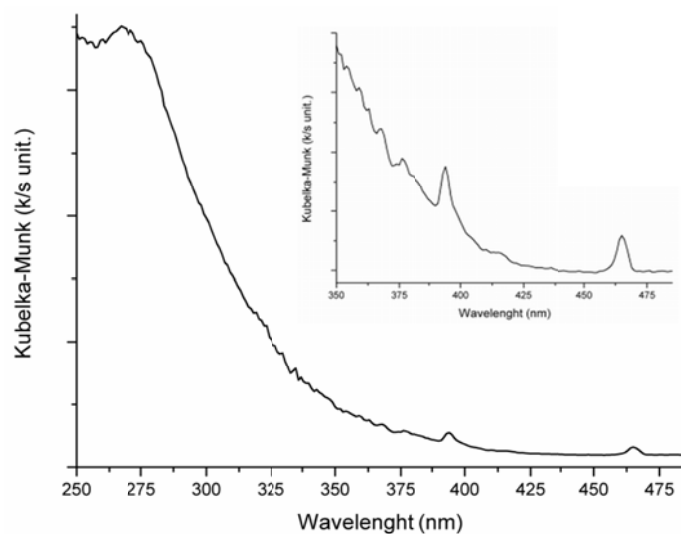


Fig. 4. Absorbance spectra of  $\text{ZnAl}_{2-x}\text{O}_4:\text{Eu}_x$

As we can see, the narrow light absorption bands of  $\text{Eu}^{3+}$  ions at 363, 380, 395, 412 and 466 nm are present.

To calculate the band gap of  $\text{ZnAl}_{2-x}\text{O}_4:\text{Eu}_x$  spinel, from absorbance spectrum we plotted  $\{(k/s)(h\nu)\}^2$  ( $\text{eV}^2$ ) vs.  $h\nu$  (Fig. 5), where  $k$  denotes absorption coefficient,  $s$  is scattering coefficient and  $h\nu$  is the photon energy.

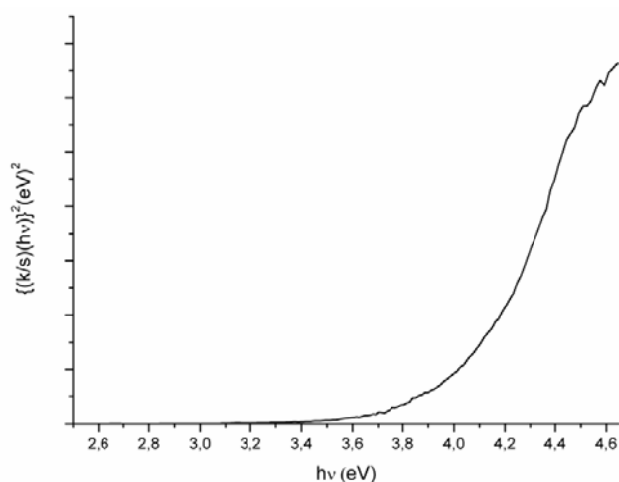


Fig. 5. Plot of  $\{(k/s)(h\nu)\}^2$  ( $\text{eV}^2$ ) vs.  $h\nu$  (energy) for  $\text{ZnAl}_{2-x}\text{O}_4:\text{Eu}_x$

The band gap was calculated by extrapolating the linear portion of the curve to  $h\nu$  equal to zero (Fig. 5) and was found to be 3.89 eV.

Excitation and emission spectra of  $\text{ZnAl}_{2-x}\text{O}_4:\text{Eu}_x$  spinel prepared by hydrothermal method are presented in Fig. 6 and 7.

Excitation spectrum of  $\text{ZnAl}_{2-x}\text{O}_4:\text{Eu}_x$  spinel was monitored at 617 nm in the range 250-485 nm. The excitation spectrum collected at room temperature at 617 nm presents similar bands as the absorbance spectra. The band centered at 253 nm is due to a charge-transfer transition from  $\text{O}^{2-}$  to  $\text{Eu}^{3+}$  ions and occurs between 250 and 300 nm [17].

The specific bands of  $\text{Eu}^{3+}$  ions appears between 350-480 nm, as we can see in Fig. 6. These bands are attributed to the transition of  $\text{Eu}^{3+}$  ions from  ${}^5\text{F}_0 \rightarrow {}^5\text{D}_4$ ,  ${}^7\text{F}_0 \rightarrow {}^5\text{L}_6$ ,  ${}^7\text{F}_0 \rightarrow {}^5\text{D}_3$  and  ${}^7\text{F}_0 \rightarrow {}^5\text{D}_2$  [18].

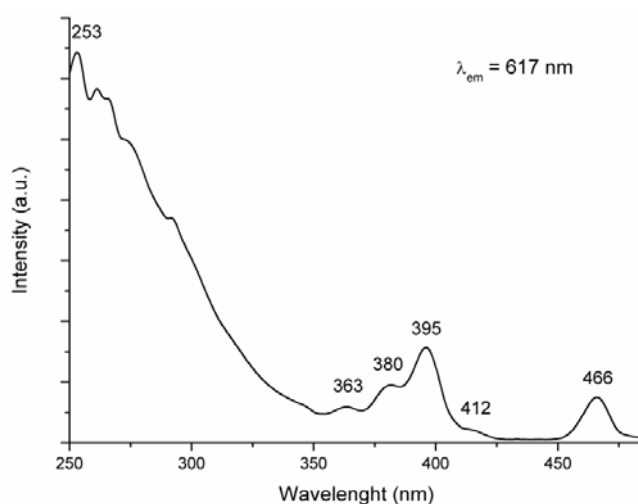


Fig. 6. Excitation spectra of  $\text{ZnAl}_{2-x}\text{O}_4:\text{Eu}_x$

Fig. 7 gives us the typical red photoluminescence spectrum of  $\text{Eu}^{3+}$  ions in the  $\text{ZnAl}_2\text{O}_4$  host monitored at (a)  $\lambda_{\text{ex}} = 395$  nm and (b)  $\lambda_{\text{ex}} = 253$  nm at the room temperature.

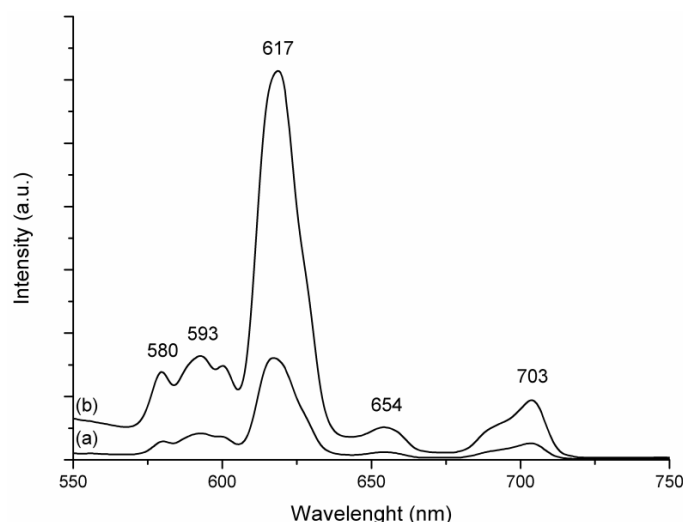


Fig. 7. Emission spectra of  $\text{ZnAl}_{2-x}\text{O}_4:\text{Eu}_x$  at (a)  $\lambda_{\text{ex}} = 395$  nm and (b)  $\lambda_{\text{ex}} = 253$  nm

As we expected, the intensity of emission spectrum monitored at  $\lambda_{\text{ex}} = 253$  nm is higher than the one monitored at  $\lambda_{\text{ex}} = 395$  nm. The emission bands that occurs between 580 and 703 nm can be assigned to the  ${}^5\text{D}_0 \rightarrow {}^7\text{F}_0$ ,  ${}^5\text{D}_0 \rightarrow {}^7\text{F}_1$ ,  ${}^5\text{D}_0 \rightarrow {}^7\text{F}_2$ ,  ${}^5\text{D}_0 \rightarrow {}^7\text{F}_3$  and  ${}^5\text{D}_0 \rightarrow {}^7\text{F}_4$  transitions. As we can see, the  ${}^5\text{D}_0 \rightarrow {}^7\text{F}_2$  red emission centered at 617 nm is the most intense which means that the  $\text{Eu}^{3+}$  ion is situated in a low symmetry environment [17].

#### 4. Conclusions

In this paper, we successfully prepared  $\text{ZnAl}_2\text{O}_4$  nanocrystals doped with  $\text{Eu}^{3+}$  ions having the normal spinel structure by hydrothermal method. X-ray diffraction analysis confirmed the high crystallinity degree of the prepared sample when using a heat treatment at  $1000^\circ\text{C}$ . The average crystallite size calculated from X-ray diffraction pattern using Scherrer's equation was smaller than 40 nm. This result was confirmed by atomic force microscopy measurements, also. The band

gap of  $\text{ZnAl}_{2-x}\text{O}_4\text{:Eu}_x$  spinel was found to be 3.89 eV and PLE measurements confirmed the high luminescent properties of the sample.

### Acknowledgement

This work was partially supported by the strategic grant POSDRU/88/1.5/S/50783, Project ID50783 (2009), co-financed by the European Social Fund – Investing in People, within the Sectorial Operational Programme Human Resources Development 2007-2013.

The authors would thank to Mihaela Birdeanu, Cornelia Bandas, Paula Sfirloaga and Daniel Ursu from National Institute for Research and Development in Electrochemistry and Condensed Matter Timisoara for Atomic force microscopy, UV-VIS-NIR, energy dispersive X-ray (EDX) and X-ray diffraction analysis.

### References

- [1] M. Vasile, P. Vlazan, A. Bucur, P. Sfirloaga, I. Grozescu, N.M. Avram, J. Optoelectron. Adv. Mater. **4**(2), 220 (2010)
- [2] Y.W. Jun, J.S. Choi, J.W. Cheon, Angew. Chem. Int. Ed. **45**, 3414 (2006)
- [3] X. Wei, D. Chen, Mater. Lett. **60**, 823 (2006)
- [4] M. Zawadzki, Solid State Sciences **8**, 14 (2006)
- [5] K. Kumar, K. Ramamoorthy, P.M. Koinkar, R. Chandramohan, K. Sankaranarayanan, J. Crystal Growth **289**, 405 (2006)
- [6] V. Ciupina, I. Carazeanu, G. Prodan, J. Optoelectron. Adv. Mater. **6**(4), 1317 (2004)
- [7] S. Farhadi, S. Panahandehjoo, Appl. Catal. A: Gen. **382**, 293 (2010)
- [8] X.Y. Chen, C. Ma, S.P. Bao, Z. Li, J. Colloid and Interface Sci. **346**, 8 (2010)
- [9] X. Y. Chen, C. Ma, Z. J. Zhang, B. N. Wang, Mater. Sci. Eng. B **151**, 224 (2008)
- [10] R.F. Martins, O.A. Serra, J. Braz. Chem. Soc. **21**(7), 1395 (2010)
- [11] S. F. Wang, F. Gu, M. K. Lü, X. F. Cheng, W. G. Zou, G. J. Zhou, S. M. Wang, Y. Y. Zhou, J. Alloys. Compd. **394**, 255 (2005)
- [12] Z. Lou, J. Hao, Thin Solid Films, **450**, 334 (2004)
- [13] M. Zawadzki, J. Wrzyszczyk, W. Streck, D. Hreniak J. Alloys. Compd. **323**, 279 (2001)
- [14] T. Minami, H. Sato, K. Ohashi, T. Tomofuji, S. Takata, J. Cryst. Growth **117**, 370 (1992)
- [15] P. Kubelka, F. Munk, Zh. Tekh. Fiz. **12**, 593 (1931)
- [16] P. Kubelka, J. Opt. Soc. Am. **38**, 448 (1948)
- [17] B. S. Barros, P. S. Melo, R. H. G. A. Kiminami, A. C. F. M. Costa, G. F. de Sá, S. Alvares Jr., J. Mater. Sci., **41**, 4744 (2006)
- [18] B. C. Cheng, S. C. Qu, H. Y. Zhou, Z. G. Wang, Nanotechnology, **17**, 2982 (2006)